VILNIUS TECH
Vilnius Gediminas Technical University

AVIATION
ISSN: 1648-7788 / eISSN: 1822-4180
2021 Volume 25 Issue 3: 202–210
https://doi.org/10.3846/aviation.2021.15663

AN ALTERNATIVE APPROACH TO INDUCED DRAG REDUCTION

Nikolaos KEHAYAS *

Department of Aeronautical Sciences, Hellenic Air Force Academy, 13671 Dekelia, Greece

Received 6 October 2020; accepted 4 March 2021

Abstract. Induced drag constitutes approximately 40% of the total drag of subsonic civil transport aircraft at cruise conditions. Various types of winglets and several non-planar concepts, such as the C-wing, the joined wings, and the box plane, have been proposed for its reduction. Here, a new approach to induced drag reduction in the form of a combination of an elliptical and an astroid hypocycloid lift distribution is put forward. Lift is mainly generated from high circulation in the center part of the wing and fades away along the semi-span towards the wing tip. Using lifting line theory, the analysis shows that for fixed lift and wingspan the combined lift distribution results in an induced drag reduction of 50% with respect to the elliptical distribution. Due to its wing planform the combined lift distribution leads to a 51.5% higher aspect ratio. If structural constraints are placed, then the higher aspect ratio may affect wing weight. Although any substantial increase of wing weight is not envisaged, further study of the matter is required. Zero-lift drag and lift-dependent drag due to skin friction and viscosity-related pressure remain unaffected. The proposed lift distribution is particularly useful in a blended wing-body design.

Keywords: drag reduction, induced drag, drag due to lift, vortex drag, lifting line theory, lift distribution.

Introduction

Fuel costs and greater awareness of the impact of emissions on the atmosphere raise the importance of fuel efficiency for future transport aircraft. Fuel consumption can be reduced by decreasing airframe weight or drag and improving the efficiency of the propulsion system (Allison et al., 2010). At subsonic speeds, aircraft drag is caused by two basic phenomena: the influence of viscosity, primary through skin friction, and losses associated with the generation of wing lift (Kroo, 2001). Induced drag is lift-depended drag as the result of trailing wing tip vortices. Induced drag accounts for nearly 40% of the total drag of subsonic civil transport aircraft at cruise conditions (Howe, 2000; Torenbeek, 2013; Kroo, 2001).

Reduced induced drag is achieved by increasing aspect ratio and/or span efficiency factor. Increasing aspect ratio decreases wing vortex strength, and hence it results in lower induced drag. The disadvantages of this approach include increased wing structural weight due to higher wing bending moments. The other option is to reduce induced drag by increasing wingspan efficiency factor. Towards this end several concepts and schemes, such as winglets (Whitcomb, 1976; Chattot, 2006; Demasi et al., 2019) and non-planar lifting surfaces in the form of the C-wing (McMasters & Kroo, 1998), the joined wings (Wolkovich, 1985) and the box wing (Prandtl, 1924; Scardaoni, 2020), have been proposed. Among them, only winglets have been used in operational aircraft. The reason is that non-planar concepts are complex and the source of problems in the overall design of aircraft (Kroo, 2001). Winglets have an induced drag reduction potential of 20 to 25% (Whitcomb, 1976; Demasi et al., 2019).

Beyond the classification according to winglet designs and non-planar concepts, publications in the field of induced drag reduction range from reviews (Kroo, 2001) to specific issues (Taylor & Hunsaker, 2020a, 2020b; Phillips et al., 2019; Demasi, 2006). Specific issues include variational approaches (Demasi, 2006) and numerical methods for design and optimization (Taylor & Hunsaker, 2020b). Another group of publications focuses on minimizing induced drag under structural constraints (Jones, 1950; Pate & German, 2013; Phillips et al., 2019; Taylor & Hunsaker, 2020a). Lately, there is a renewed interest in Prandtl's box wing (Prandtl, 1924) as the lifting system with minimum induced drag (Frediani & Montanari, 2009; Cavallaro & Demasi, 2016; Scardaoni, 2020).

Lift distributions of plain planar wings for fixed lift and wingspan without any further constraints generating less

*Corresponding author. E-mail: *n.kehayas@gmail.com*

induced drag than Prandtl's (1921) elliptical distribution are not known.

In the present study a new approach in the shape of a combination of an elliptical and an astroid hypocycloid lift distribution is put forward with the objective to reduce induced drag. The motivation is to find a way to decrease induced drag of plain planar wings simpler and more effective than existing non-planar concepts or winglet designs. The elliptical lift distribution spans the center part and the astroid hypocycloid the outer parts of the wing. This combined distribution reduces wing vortices by smoothly fading away lift towards the wing tip. Although most of the lift is provided by the elliptical distribution in the center part of the wing, the astroid hypocycloid distribution in the outer parts of the wing contributes to lift as well. Following lifting line theory, the induced drag of the proposed combined lift distribution is evaluated, and then compared with the induced drag of the elliptical lift distribution, non-planar concepts, and winglet designs. The proposed lift distribution is examined as to its application to aircraft design.

1. Analysis

It has been shown by Prandtl's lifting line theory that the lift distribution which yields the minimum induced drag for fixed lift and wingspan is the elliptical lift distribution (Anderson, 1984). This is the minimum vortex drag and does not include lift-dependent drag due to skin friction and viscosity-related pressure drag (Kroo, 2001). The induced drag coefficient of wings with an elliptical lift distribution is given by

$$C_{di} = \frac{C_l^2}{\pi AR}. \tag{1}$$

The proposed combined lift distribution is shown in Figure 1. The two lift distributions blend at the point where they have the same gradient and value of circulation. Further down in the analysis this point is found to be $0.71(b_e/2)$, $0.71(b_a/2)$, where $b_e/2$ and $b_a/2$ are respectively the elliptical and the astroid hypocycloid distributions semi-spans. The elliptical part of the combined lift distribution spans from the origin of the semi-span of the combined lift distribution, 0_c, to the blending point of the two distributions, $0.71(b_e/2)$, $0.71(b_a/2)$, and the astroid hypocycloid part spans from the blending point, $0.71(b_e/2)$, $0.71(b_a/2)$, to the end of the semi-span of the combined distribution, $b/2$.

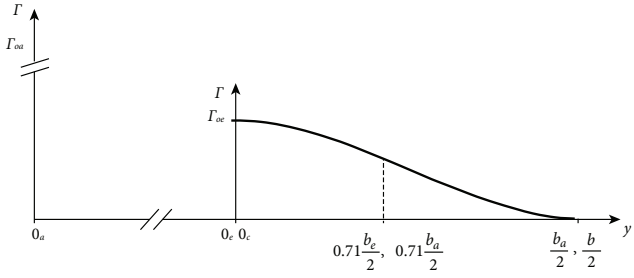

Figure 1. Combination of an elliptical and an astroid hypocycloid lift (circulation) distribution

The following analysis applies to vortex drag of unswept, untwisted plain planar wings for fixed lift and wingspan without any other constraints in incompressible flow.

For an elliptical lift distribution (Anderson, 1984) along the span of the wing, the circulation distribution, $\Gamma_e(y)$, is given by

$$\Gamma_e(y) = \Gamma_{oe}\left(1-\left(\frac{y}{(b_e/2)}\right)^2\right)^{(1/2)}, \tag{2}$$

where y is the distance along the wing semi-span and $b_e/2$ is the semi-span of the wing based on an elliptical lift distribution.

For an astroid hypocycloid (Simmons, 1992) lift distribution along the span of the wing, the circulation distribution, $\Gamma_a(y)$, is given by

$$\Gamma_a(y) = \Gamma_{oa}\left(1-\left(\frac{y}{(b_a/2)}\right)^{(2/3)}\right)^{(3/2)}, \tag{3}$$

where y is the distance along the wing semi-span and $b_a/2$ is the semi-span of the wing based on an astroid hypocycloid lift distribution.

As already mentioned and shown in Figure 1, the elliptical lift distribution covers the center part and the astroid hypocycloid the outer parts of the wing. The two lift distributions blend at the point where they have the same gradient and value of circulation. For the same circulation gradient

$$\frac{d\Gamma_e}{dy} = \frac{d\Gamma_a}{dy}. \tag{4}$$

For an elliptical circulation distribution with a minor to major semi-axis ratio of 1/2 we have

$$\frac{\Gamma_{oe}}{(b_e/2)} = 0.5 \tag{5}$$

and for an astroid hypocycloid circulation distribution with an axial ratio of 1 we have

$$\frac{\Gamma_{oa}}{(b_a/2)} = 1. \tag{6}$$

Let

$$y = Y\frac{b_e}{2} = Y\frac{b_a}{2}. \tag{7}$$

Use of equations (2) and (3) to evaluate equation (4) and then substituting equations (5), (6) and (7) into it gives

$$1 - Y^{(2/3)} - Y^2 + 0.75Y^{(8/3)} = 0, \tag{8}$$

whose solution is $Y = \pm 0.71$.

The two distributions do not have the same origin in the y (wingspan) axis and the blending point is located at

$$\pm 0.71\frac{b_e}{2}, \pm 0.71\frac{b_a}{2}.$$

For the same circulation value at the blending point

$$\Gamma_e = \Gamma_a. \tag{9}$$

Use of equations (2), (3), (8) and (9) gives

$$\frac{\Gamma_{oe}}{\Gamma_{oa}}=\frac{\left(1-Y^{(2/3)}\right)^{(3/2)}}{\left(1-Y^{2}\right)^{(1/2)}}, \tag{10}$$

whose solution satisfying blending point values of

$$y=\pm 0.71\frac{b_e}{2} \quad \text{or} \quad y=\pm 0.71\frac{b_a}{2} \quad \text{is}$$

$$\Gamma_{oa}=7.636\Gamma_{oe}. \tag{11}$$

Hence, from equations (5), (6) and (11)

$$\left(\frac{b_e}{2}\right)=2\frac{\Gamma_{oa}}{7.636}; \tag{12}$$

$$\left(\frac{b_e}{2}\right)=\frac{1}{3.818}\left(\frac{b_a}{2}\right). \tag{13}$$

From the above, as indicated in Figure 1, the semi-span of the combination of the two lift distributions, *b/2*, is

$$\left(\frac{b}{2}\right)=0.71\left(\frac{b_e}{2}\right)+0.29\left(\frac{b_a}{2}\right) \tag{14}$$

and using equation (13)

$$\left(\frac{b}{2}\right)=1.818\left(\frac{b_e}{2}\right). \tag{15}$$

According to Anderson (1984) induced velocity, $w(y_o)$, which is the cause of induced drag, is given by

$$w\left(y_0\right)=-\left(\frac{1}{4\pi}\right)\int_{-b/2}^{b/2}\left(\left(\frac{d\Gamma}{dy}\right)\left(\frac{1}{\left(y_0-y\right)}\right)\right)dy. \tag{16}$$

But

$$w\left(y_0\right)=w\left(y_0\right)_e+w\left(y_0\right)_{a1}+w\left(y_0\right)_{a2}, \tag{17}$$

where

$$w\left(y_0\right)_e=$$
$$-\left(\frac{1}{4\pi}\right)\int_{-0.71b_e/2}^{0.71b_e/2}\left(\left(\frac{d\Gamma_e}{dy}\right)\left(\frac{1}{\left(y_0-y\right)}\right)\right)dy \tag{18}$$

is the induced velocity due to the elliptical lift distribution of the central part of the wing, and

$$w\left(y_0\right)_{a1}=$$
$$-\left(\frac{1}{4\pi}\right)\int_{0.71b_a/2}^{b_a/2}\left(\left(\frac{d\Gamma_a}{dy}\right)\left(\frac{1}{\left(y_0-y\right)}\right)\right)dy; \tag{19}$$

$$w\left(y_0\right)_{a2}=$$
$$-\left(\frac{1}{4\pi}\right)\int_{-0.71b_a/2}^{-b_a/2}\left(\left(\frac{d\Gamma_a}{dy}\right)\left(\frac{1}{\left(y_0-y\right)}\right)\right)dy \tag{20}$$

are the induced velocities due to the astroid hypocycloid lift distribution of the outer parts of the wing.

To continue with the evaluation of the integrals for the induced velocity and lift, a transformation of variables is needed (Anderson, 1984). It is the transformation of the linear variable of the distance along the semi-span, *y*, into an angle variable, θ, with respect to the corresponding lift distributions semi-spans, $b_e/2$ and $b_a/2$. The reason is to facilitate the evaluation of these integrals, especially the induced velocity integral of the elliptic lift distribution.

For the induced velocity, w_e, due to the elliptical part of the lift distribution, by using equation (2), we have

$$w\left(y_0\right)_e=-\left(\frac{\Gamma_{oe}}{\left(\pi b^2\right)}\right)$$
$$\int_{-0.71b_e/2}^{0.71b_e/2}\left(\left(\frac{y}{\left(1-\left(y/b\right)^2\right)^{(1/2)}}\right)\left(\frac{1}{\left(y_0-y\right)}\right)\right)dy. \tag{21}$$

Considering the transformation of the distance along the semi-span variable, *y*, into an angle variable, θ, for an elliptical distribution, the following substitution is applied

$$y=\left(\frac{b_e}{2}\right)\cos\theta, \quad dy=-\left(\frac{b_e}{2}\right)\sin\theta d\theta.$$

At

$$0.71\frac{b_e}{2}=\left(\frac{b_e}{2}\right)\cos\theta, \quad \theta=0.75\pi$$

and at

$$-0.71\frac{b_e}{2}=\left(\frac{b_e}{2}\right)\cos\theta, \quad \theta=0.25\pi. \tag{22}$$

(For clarity purposes angle limits are rounded to the second decimal place, resulting in an error of less than 1%).

Hence,

$$w\left(\theta_0\right)_e=$$
$$-\left(\frac{\Gamma_{oe}}{\left(2\pi b_e\right)}\right)\int_{0.25\pi}^{0.75\pi}\left(\frac{\cos\theta}{\left(\cos\theta-\cos\theta_0\right)}\right)d\theta. \tag{23}$$

To evaluate induced velocity, equation (23), use of the Glauert Integral (GI) (Glauert, 1947) is made. Therefore,

$$\int_{0.25\pi}^{0.75\pi}\left(\frac{\cos\theta}{\left(\cos\theta-\cos\theta_o\right)}\right)d\theta=0.50\pi \tag{24}$$

and hence,

$$w_e=-0.50\frac{\Gamma_{oe}}{\left(2b_e\right)}. \tag{25}$$

For the induced velocity, w_a, due to the astroid hypocycloid parts of the lift distribution, using equation (3), we have

$$w\left(y_0\right)_{a1}=\frac{\Gamma_{oa}}{\left(4\pi\left(b_a/2\right)^{(2/3)}\right)}$$
$$\int_{0.71b_a/2}^{b_a/2}\left(\left(1-\left(y/b_a\right)^{(2/3)}\right)^{(1/2)}\right)$$

$$\left(\frac{1}{\left(\left(y^{(1/3)}\right)\left(y_0-y\right)\right)}\right)dy. \quad (26)$$

Considering the transformation of the distance along the semi-span variable, y, into an angle variable, θ, for an astroid hypocycloid distribution, the following substitution is applied

$$y=\left(\frac{b_a}{2}\right)\cos^3\theta,\ \ dy=-\left(\frac{b_a}{2}\right)3\cos^2\theta\sin\theta d\theta. \quad (27)$$

At

$$0.71\frac{b_a}{2}=\left(\frac{b_a}{2}\right)\cos^3\theta,\ \ \theta=0.15\pi$$

and at

$$-0.71\frac{b_a}{2}=\left(\frac{b_a}{2}\right)\cos^3\theta,\ \ \theta=0.85\pi. \quad (28)$$

(For clarity purposes angle limits are rounded to the second decimal place, resulting in an error of less than 1%).

Consequently,

$$w\left(\theta_0\right)_{a1}=$$

$$-\left(\frac{\Gamma_{oa}}{\left(2\pi b_a\right)}\right)\int_0^{0.15\pi}\left(\frac{\left(3\sin^2\theta\cos\theta\right)}{\left(\cos^3\theta-\cos^3\theta_o\right)}\right)d\theta; \quad (29)$$

$$w\left(\theta_0\right)_{a2}=$$

$$-\left(\frac{\Gamma_{oa}}{\left(2\pi b_a\right)}\right)\int_{0.85\pi}^{\pi}\left(\frac{\left(3\sin^2\theta\cos\theta\right)}{\left(\cos^3\theta-\cos^3\theta_o\right)}\right)d\theta. \quad (30)$$

Or, using equations (11) and (13)

$$w\left(\theta_0\right)_{a1}=$$

$$-\left(\frac{7.636\Gamma_{oe}}{\left(2\pi 3.818 b_e\right)}\right)\int_0^{0.15\pi}\left(\frac{\left(3\sin^2\theta\cos\theta\right)}{\left(\cos^3\theta-\cos^3\theta_o\right)}\right)d\theta; \quad (31)$$

$$w\left(\theta_0\right)_{a1}=$$

$$-\left(\frac{\Gamma_{oe}}{\left(\pi b_e\right)}\right)\int_0^{0.15\pi}\left(\frac{\left(3\sin^2\theta\cos\theta\right)}{\left(\cos^3\theta-\cos^3\theta_o\right)}\right)d\theta. \quad (32)$$

At

$$y=\pm 0.71\frac{b_e}{2},\ \ \pm 0.71\frac{b_a}{2}$$

$$\frac{d\Gamma_a}{dy}=\frac{d\Gamma_e}{dy},\ \ \Gamma_a=\Gamma_e. \quad (33)$$

Therefore, at

$$y=+0.71\frac{b_e}{2}$$

or

$$y=+0.71\frac{b_a}{2}$$

using equations (23), (24), (32) and (33)

$$-\left(\frac{\Gamma_{oe}}{\left(\pi b_e\right)}\right)\left(\frac{\left(3\sin^2\theta\cos\theta\right)}{\left(\cos^3\theta-\cos^3\theta_o\right)}\right)=-\left(\frac{\Gamma_{oe}}{\left(2\pi b_e\right)}\right). \quad (34)$$

At

$$y=+\frac{b_a}{2},\ \ y=+\frac{b}{2}$$

$$\frac{d\Gamma_a}{dy}=0,\ \ \Gamma_a=0.$$

Hence,

$$-\left(\frac{\Gamma_{oe}}{\left(\pi b_e\right)}\right)\left(\frac{\left(3\sin^2\theta\cos\theta\right)}{\left(\cos^3\theta-\cos^3\theta_o\right)}\right)=0. \quad (35)$$

Figure 2 presents the variation of downwash gradient with wingspan in terms of wingspan variable transformation angle, θ, for every angle of point of downwash, θ_o. The downwash gradient of the elliptical part of the combined lift distribution spans from the origin of the semi-span, 0.5π, to the blending point, 0.25π, 0.15π (0.71(b_e/2),0.71(b_a/2)), and the astroid hypocycloid part from the blending point, 0.25π, 0.15π (0.71(b_e/2), 0.71(b_a/2)), to the end of the semi-span of the combined distribution, 0.

Numerically integrating by equation (32) from 0.15π to 0, considering equations (34) and (35) (Figure 2), gives

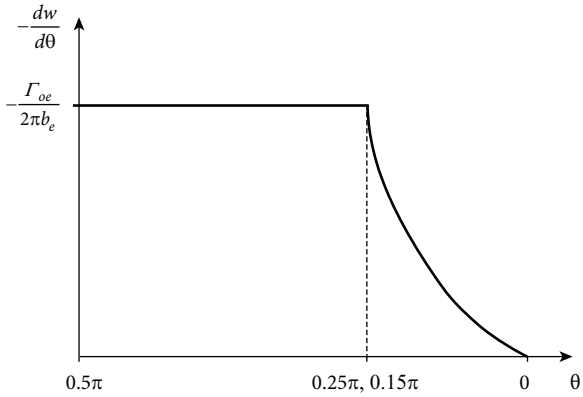

Figure 2. Variation of downwash gradient with wingspan in terms of wingspan variable transformation angle, θ, for every angle of point of downwash, θ_o

$$w_{a1}=-0.05\left(\frac{\Gamma_{oe}}{\left(2b_e\right)}\right). \quad (36)$$

Similarly,

$$w_{a2}=-0.05\left(\frac{\Gamma_{oe}}{\left(2b_e\right)}\right). \quad (37)$$

Hence,

$$w_a=w_{a1}+w_{\alpha 2}; \quad (38)$$

$$w_a=-0.10\left(\frac{\Gamma_{oe}}{\left(2b_e\right)}\right). \quad (39)$$

For the lift, L_e, due to the elliptical part of the distribution we have

$$L_e = \rho_\infty V_\infty \Gamma_{oe} \int_{-0.71b_e/2}^{0.71b_e/2} \left(1-\left(\frac{y}{(b_e/2)}\right)^2\right)^{(1/2)} dy. \quad (40)$$

Considering the transformation of the distance along the semi-span variable, y, into an angle variable, θ, for an elliptical distribution, the following substitution is applied

$$y = \left(\frac{b_e}{2}\right)\cos\theta, \; dy = -\left(\frac{b_e}{2}\right)\sin\theta d\theta; \quad (41)$$

$$L_e = \rho_\infty V_\infty \Gamma_{oe}(b_e/2) \int_{0.25\pi}^{0.75\pi} \sin^2\theta d\theta \quad (42)$$

and hence,

$$L_e = \rho_\infty V_\infty 0.8185 \Gamma_{oe} \frac{b_e}{4}\pi. \quad (43)$$

For the lift, L_a, due to the astroid hypocycloid part of the distribution we have

$$L_a = \rho_\infty V_\infty \Gamma_{oa} \frac{b_a}{2}\left(\int_{0.71b_a/2}^{b_a/2} \left(1-\frac{y}{(b_a/2)}\right)^{(3/2)} dy + \int_{-0.71b_a/2}^{-b_a/2} \left(1-\frac{y}{(b_a/2)}\right)^{(3/2)} dy \right). \quad (44)$$

Considering the transformation of the distance along the semi-span variable, y, into an angle variable, θ, for an astroid hypocycloid distribution, the following substitution is applied

$$y = \left(\frac{b_a}{2}\right)\cos^3\theta, \; dy = -\left(\frac{b_a}{2}\right)3\cos^2\theta\sin\theta d\theta. \quad (45)$$

Therefore,

$$L_a = \rho_\infty V_\infty \Gamma_{oa} \frac{b_a}{2} \left(\int_0^{0.15\pi} \left(1-\cos^2\theta\right)^{(3/2)} 3\cos^2\theta\sin\theta d\theta + \int_{0.85\pi}^{\pi} \left(1-\cos^2\theta\right)^{(3/2)} 3\cos^2\theta\sin\theta d\theta \right). \quad (46)$$

According to Simmons (1992)

$$\Gamma_{oa}\frac{b_a}{2}\int_0^{0.15\pi}\left(1-\cos^2\theta\right)^{(3/2)}3\cos^2\theta\sin\theta d\theta = \frac{3}{16}\Gamma_{oa}\frac{b_a}{2}\left(\theta-\frac{\sin 4\theta}{4}\right)_0^{0.15\pi} - \frac{3}{8}\Gamma_{oa}\frac{b_a}{2}\left(\frac{\left(\sin^3 2\theta\right)}{6}\right)_0^{0.15\pi}. \quad (47)$$

Consequently,

$$\Gamma_{oa}\frac{b_a}{2}\int_0^{0.15\pi}\left(1-\cos^2\theta\right)^{(3/2)}3\cos^2\theta\sin\theta d\theta = 0.00655\Gamma_{oa}\frac{b_a}{4}\pi. \quad (48)$$

Similarly,

$$\Gamma_{oa}\frac{b_a}{2}\int_{0.85\pi}^{\pi}\left(1-\cos^2\theta\right)^{(3/2)}3\cos^2\theta\sin\theta d\theta = 0.00655\Gamma_{oa}\frac{b_a}{4}\pi. \quad (49)$$

Hence, using equation (46)

$$L_a = \rho_\infty V_\infty 0.0131\Gamma_{oa}\frac{b_a}{4}\pi. \quad (50)$$

Next, in order to find the downwash, w, and the lift, L, of the combined elliptical and astroid hypocycloid lift distribution, the downwash, w, and the lift, L, for each distribution must be reduced to the span, b, of the combined distribution.

Using the definition of induced velocity equations (15) and (25) the reduced downwash of the elliptical part, w_{ec}, is

$$w_{ec} = -0.50\frac{\Gamma_{oe}}{(2\cdot 1.818b)} = -0.2750\frac{\Gamma_{oe}}{2b} \quad (51)$$

and using the definition of induced velocity equations (15) and (39) the reduced downwash of the astroid hypocycloid part, w_{ac}, is

$$w_{ac} = -0.10\frac{\Gamma_{oe}}{(2\cdot 1.818b)} = -0.0550\frac{\Gamma_{oe}}{2b}. \quad (52)$$

Hence, the downwash of the combined distribution is

$$w = w_{ec} + w_{ac} = -0.33\frac{\Gamma_{oe}}{2b}. \quad (53)$$

Using equations (15) and (43) the reduced lift of the elliptical part, L_{ec}, is

$$L_{ec} = \rho_\infty V_\infty 0.8185\Gamma_{oe}\frac{b}{(4\cdot 1.818)}\pi; \quad (54)$$

$$L_{ec} = \rho_\infty V_\infty 0.4502\Gamma_{oe}\frac{b}{4}\pi \quad (55)$$

and using equations (11), (13), (15) and (50) the reduced lift of the astroid hypocycloid part, L_{ac}, is

$$L_{ac} = \rho_\infty V_\infty 0.0131\cdot 7.636\Gamma_{oe}\frac{3.818}{1.818}\frac{b}{4}\pi; \quad (56)$$

$$L_{ac} = \rho_\infty V_\infty \Gamma_{oe} 0.2101\frac{b}{4}\pi. \quad (57)$$

Therefore, the lift of the combined distribution is

$$L = L_{ec} + L_{ac} = \rho_\infty V_\infty 0.66\frac{\Gamma_{oe}\cdot b}{4}\pi. \quad (58)$$

Further, according to Anderson (1984) the induced angle, a_i, is given by

$$\alpha_i = -\left(\frac{w}{V_\infty}\right) \quad (59)$$

and using equation (53)

$$\alpha_i = 0.33\frac{\Gamma_{oe}}{\left(V_\infty b\right)}. \tag{60}$$

From equation (58)

$$\Gamma_{oe} = \frac{4L}{\left(\rho_\infty V_\infty b\pi 0.66\right)}. \tag{61}$$

But,

$$L = C_l \frac{1}{2}\rho_\infty V_\infty^2 S. \tag{62}$$

Hence,

$$\Gamma_{oe} = \frac{\left(2V_\infty S C_l\right)}{\left(b\pi 0.66\right)}. \tag{63}$$

Substituting equation (63) into equation (60) gives

$$\alpha_i = \frac{0.33}{0.66}\frac{C_l S}{\pi b^2} = 0.50\frac{C_l}{\pi AR}. \tag{64}$$

According to Anderson (1984) the induced drag coefficient, C_{di}, follows from induced drag, D_i, given by

$$D_i = \int_{-b/2}^{b/2} L(y)\alpha_i(y)dy. \tag{65}$$

Using equation (64)

$$D_i = \alpha_i L \tag{66}$$

and

$$C_{di} = \frac{\alpha_i}{\left((1/2)\rho_\infty V_\infty^2 S\right)}\rho_\infty V_\infty \int_{-b/2}^{b/2} \Gamma(y)dy. \tag{67}$$

Using equation (58)

$$C_{di} = \frac{\alpha_i}{\left((1/2)\rho_\infty V_\infty^2 S\right)}\rho_\infty V_\infty \Gamma_{oe}\frac{b}{4}\pi 0.66. \tag{68}$$

Substituting equations (63) and (64) into equation (68) we have

$$C_{di} = \frac{\frac{0.50C_l}{\left(\pi AR\right)}}{\left((1/2)\rho_\infty V_\infty^2 S\right)}\rho_\infty V_\infty \frac{\left(2V_\infty S C_l\right)}{\left(b\pi 0.66\right)}\frac{b}{4}\pi 0.66. \tag{69}$$

Finally,

$$C_{di} = 0.50\frac{C_l^2}{\pi AR} \tag{70}$$

and

$$D_i = 0.50\frac{C_l^2}{\pi AR}\frac{1}{2}\rho_\infty V_\infty^2 S \tag{71}$$

or

$$D_i = 0.50\frac{C_l^2}{\pi b^2}\frac{1}{2}\rho_\infty V_\infty^2 S^2. \tag{72}$$

To be possible to compare the induced drag found for the combined elliptical and astroid hypocycloid lift distribution (equation (72)) with the induced drag of the elliptical lift distribution for the same lift and wingspan, the above result (equation(72)) must be further examined.

Keeping all other parameters constant, the wing surface (planform), and consequently the lift of the combined elliptical and astroid hypocycloid lift distribution is 66% of the elliptical (equation (58)). To compare the induced drag of the combined lift distribution with the elliptical for the same lift and wingspan, the lift of the combined distribution must be brought up to the level of the lift of the elliptical. For the same wingspan, the combined lift distribution has a wing surface which is 66% that of the elliptical. Consequently, for the same lift and wingspan the lift coefficient (circulation) of the combined, C_{lc}, must be increased by 51.5 % with respect to the elliptical, C_{le} (1.515 × 0.66 = 1.00).

Using the subscripts *c* for the combined and *e* for the elliptical

$$D_{ic} = 0.50\frac{{C_{lc}}^2}{\pi b_c^2}\frac{1}{2}\rho_\infty V_\infty^2 S_c^2, \tag{73}$$

where

$$C_{lc} = 1.515 C_{le}; \tag{74}$$

$$b_c = b_e; \tag{75}$$

$$S_c = 0.66 S_e. \tag{76}$$

By substituting equations (74)–(76) into equation (73) we have

$$D_{ic} = 0.50\frac{(1.515C_{le})^2}{\pi b_e^2}\frac{1}{2}\rho_\infty V_\infty^2\left(0.66S_e\right)^2. \tag{77}$$

Therefore,

$$D_{ic} = 0.50\frac{{C_{le}}^2}{\pi b_e^2}\frac{1}{2}\rho_\infty V_\infty^2 {S_e}^2 \tag{78}$$

and

$$D_{ic} = 0.50\, D_{ie}. \tag{79}$$

2. Results and discussion

As shown in the analysis the use of a combined elliptical and astroid hypocycloid lift distribution results in an induced drag coefficient reduction of 50% (equation(70)). This reduction translates into a span efficiency factor, *e*, of 2. At this value the combined lift distribution outperforms all non-planar concepts (Kroo, 2001). In most cases the effect is more pronounced if total drag and lift-to-drag ratio are considered. In addition, the proposed combined lift distribution is free of the design problems experienced by non-planar aircraft configurations.

The induced drag coefficient reduction of the combined elliptical and astroid hypocycloid lift distribution is two and a half times the reduction achieved by winglets (Whitcomb, 1976). The most elaborate winglet designs, such as the box winglets (Demasi et al., 2019), exhibit span efficiency factors of less than 1.5. Again, as with most non-planar concepts, the reduction is even greater if total drag and lift-to-drag ratio are considered. Winglets reduce induced drag, but they produce little lift. In contrast, the astroid hypocycloid part of the combined lift

distribution generates nearly one-third of the total lift but only one-sixth of the total downwash (Table 1). That is, in relation to the elliptical part it produces with respect to lift proportionally less downwash.

Although with the lift-to-downwash ratio as the criterion the astroid hypocycloid is more efficient than the elliptical part of the combined distribution, both, as indicated in Table 1, are more efficient than the elliptical. Not only combined, but "separately" as well they are more efficient in relation to lift-to-downwash ratio. And this effect is not due to their respective distributions but due to the section of each distribution used and its wingspan location.

The comparison of the proposed combined lift distribution with non-planar concepts and winglet designs is based on an overall height to span ratio of 0.2. For values of this ratio beyond 0.5, box plane, biplane and winglet concept performance is comparable to the combined lift distribution in terms of span efficiency factor (Kroo, 2001). However, this is only a theoretical consideration because at these overall height to span ratios these concepts exhibit serious drawbacks in relation to profile drag, structural weight, stability, and other aircraft design issues (Torenbeek, 2013).

For fixed lift and wingspan, the use of a combined elliptical and astroid hypocycloid lift distribution results in an induced drag reduction of 50% compared with the elliptical (equation (79)). The physical interpretation of this reduction is that lift is mainly produced from high circulation in the center part of the wing and fades away along the semi-span towards the wing tip. Therefore, the vortices produced by the wing are weaker. It is the outcome of replacing the elliptical lift distribution in the outer parts of the wing with the more efficient lift-to-downwash ratio astroid hypocycloid.

Fixed lift and wingspan is the established way to compare different lift distributions. Prandtl (1921) in his lifting line theory demonstrated that the lift distribution which yields the minimum induced drag for fixed lift and wingspan is the elliptical. Prandtl (1921, p. 191), states that various lift distributions were attempted, and that the elliptical gave the desired solution. He does not indicate a mathematical process towards this solution. Munk (1923, p. 7), using calculus of variations arrived at the conclusion that the necessary condition for the minimum of the induced drag is that the downwash produced to be constant along the entire lifting line.

Although the result reached in the analysis is rather unconventional, nowhere, at least not in Prandtl's (1921) and Munk's (1923) work, there is a method for deducing that the elliptical lift distribution minimizes induced drag. If a "trial and error" approach was used by Prandtl (1921) to discover the elliptical as the distribution of least induced drag, it is highly unlikely that every form of lift distribution or combination of lift distributions was investigated. Munk's (1923) finding that the downwash must be constant does not define the form of the lift distribution. The fact that the elliptical lift distribution produces a constant downwash confirms that it is the distribution producing the minimum of induced drag and not the other way around. Equally, the general lift distribution expressed as a Fourier sine series (Prandtl, 1921) implies with its first term by definition an elliptical distribution.

In the analysis by means of a numerical integration a constant downwash is reached for the astroid hypocycloid part of the combined lift distribution (equation (37)). Downwash is estimated in a numerical manner due to the great difficulty in evaluating the integral of the downwash for the astroid hypocycloid part (equation (32)). But the downwash gradient of the astroid hypocycloid part, $-dw/d\theta$, can be very closely described in the domain of its values $[0.15\pi - 0]$ by the function

$$-\frac{dw}{d\theta} = -(\Gamma_{oe} / 2\pi b_e)\left(\frac{\theta}{-0.15\pi}\right)^2, \tag{80}$$

whose integration from 0.15π to 0 gives for the astroid hypocycloid part downwash the same value analytically as numerically. That is

$$w = -0.05\left(\frac{\Gamma_{oe}}{(2b_e)}\right). \tag{81}$$

Consequently, it is shown analytically, albeit in an indirect way, that downwash is independent of the position at which it is induced, and thus it is constant over the domain $[0.15\pi - 0]$ of the astroid hypocycloid part. Hence, both elliptical and astroid hypocycloid parts of the combined lift distribution fulfill the condition of constant downwash in their respective domains of wingspan. Therefore, it may be claimed that the use of a combination

Table 1. Relative values of lift and downwash for the elliptical and the combined elliptical and astroid hypocycloid lift distributions

Lift of the elliptical distribution	Lift of the combined distribution	Lift of the elliptical part of the combined distribution	Lift of the astroid hypocycloid part of the combined distribution
1	0.660	0.450	0.210
Downwash of the elliptical distribution	Downwash of the combined distribution	Downwash of the elliptical part of the combined distribution	Downwash of the astroid hypocycloid part of the combined distribution
1	0.330	0.275	0.055

of lift distributions, elliptical and astroid hypocycloid, generates the least induced drag.

For fixed lift and wingspan, the combined elliptical and astroid hypocycloid lift distribution results in an induced drag reduction of 50% in comparison with the elliptical. If structural considerations like wing root bending moment are included in the comparison, then a different outcome arises. This is not the outcome reached by Prandtl (1933) or of any similar investigations involving structural constraints. The reason is that the planform of the combined elliptical and astroid hypocycloid lift distribution, with its large center wing area section due to its elliptical part and its small outer wing area sections due to its astroid hypocycloid part (a reflection of Figure 1), is unlike any other. This planform gives rise to a 51.5% higher aspect ratio in comparison with the elliptical. But structural effects due to a higher aspect ratio are not as adverse as they seem since the small outer wing area sections generate only one-third of the total lift (Table 1). If structural or other constraints are placed, such as bending moments, wing weight, maximum stress, wing loading and wing deflection (Phillips et al., 2019), further study of the proposed combined lift distribution is required which is beyond the scope of this paper.

The above results and discussion refer to vortex drag of plain planar wings without twist or sweep. Nevertheless, induced drag includes, even though very much smaller than vortex drag, a lift-dependent drag due to skin friction and viscosity-related pressure (Kroo, 2001). This term is related to airfoil shape and not to wing lift distribution. In this sense it is irrelevant to this analysis. But it should be noted that because of the considerable vortex-dependent drag reduction of the combined lift distribution, lift-dependent drag due to skin friction and viscosity-related pressure may now be almost in the same order of magnitude as vortex-dependent drag.

The proposed combined lift distribution could be of much use in a blended wing-body design (Kehayas, 1998). The elliptical part of the combined lift distribution could be applied to the passenger-carrying large wing area center section, and the astroid hypocycloid to the small outer wing sections of the blended wing-body. Use of lift and propulsion integration schemes (Kehayas, 2006, 2011) would more than alleviate any wing weight penalties resulting from the higher aspect ratio of the combined lift distribution.

Conclusions

The main conclusion is that the proposed combination of an elliptical and an astroid hypocycloid lift distribution for fixed lift and wingspan planar wings without any other constraints leads to an induced drag reduction of 50% in comparison with the elliptical. The physical interpretation of this reduction is that lift is mainly produced from high circulation in the center part of the wing and fades away along the semi-span towards the wing tip reducing wing vortices. Compared to the elliptical part of the combination the astroid hypocycloid generates with respect to lift proportionally less downwash. The induced drag reduction of the combined lift distribution is not due to the elliptic and the astroid hypocycloid distributions it is made from, but due to the section of each distribution used and to its wingspan location. The proposed lift distribution outperforms all non-planar concepts and winglet designs with a feasible overall height to span ratio. The wing planform of the combined lift distribution exhibits a 51.5% higher aspect ratio. If structural constraints are placed, then the higher aspect ratio may affect wing weight. Although any substantial increase in wing weight is not envisaged, further study of the matter is required. Zero-lift drag and lift-dependent drag due to skin friction and viscosity-related pressure remain unaffected. The proposed lift distribution is particularly useful in a blended wing-body design.

Disclosure statement

The author declares not to have any competing financial, professional, or personal interests from other parties.

References

Allison, E., Kroo, I., Sturdza, P., Suzuki, Y., & Martins-Rivas, H. (2010). Aircraft conceptual design with natural laminar flow. In *Proceedings of the 27th International Congress of Aeronautical Sciences* (pp. 1–9). Nice, France.

Anderson, J. D. (1984). *Fundamentals of aerodynamics*. McGraw-Hill.

Cavallaro, R., & Demasi, L. (2016). Challenges, ideas, and innovations of joined-wing configurations: a concept from the past, an opportunity for the future. *Progress in Aerospace Sciences, 87*, 1–93. https://doi.org/10.1016/j.paerosci.2016.07.002

Chattot, J.-J. (2006). Low speed design and analysis of wing/winglet combinations including viscous effects. *AIAA Journal of Aircraft*, *43*(2), 386–389. https://doi.org/10.2514/1.15349

Demasi, L. (2006). Induced drag minimization: a variational approach using the acceleration potential. *AIAA Journal of Aircraft, 43*(3), 669–680. https://doi.org/10.2514/1.15982

Demasi, L., Monegato, G., Cavallaro, R., & Rybarczyk, R. (2019). Optimum induced drag of wingtip devices: the concept of best winglet design. In *AIAA SciTech Forum* (pp. 1–48). San Diego, California. https://doi.org/10.2514/6.2019-2301

Frediani, A., & Montanari, G. (2009). Best wing system: an exact solution of the Prandtl's problem. In G. Buttazzo & A. Frediani (Eds.), *Variational analysis and aerospace engineering* (pp. 183–211). Springer. https://doi.org/10.1007/978-0-387-95857-6_11

Glauert, H. (1947). *The Elements of aerofoil and airscrew theory* (2nd ed.). Cambridge University Press.

Howe, D. (2000). *Aircraft conceptual design synthesis*. Professional Engineering Publishing Limited. https://doi.org/10.1002/9781118903094

Jones, R. T. (1950). *The spanwise distribution of lift for minimum induced drag of wings having a given lift and a given bending moment.* NASA TN-2249.

Kehayas, N. (1998). The blended wing-body configuration as an alternative to conventional subsonic civil transport aircraft design. In *Proceedings of the 21st International Congress of Aeronautical Sciences* (pp. 1–7). Melbourne, Australia.

Kehayas, N. (2006). A powered lift design for subsonic civil transport aircraft. In *Proceedings of the 25th International Congress of Aeronautical Sciences* (pp. 1–10). Hamburg, Germany.

Kehayas, N. (2011). Propulsion system of a jet-flapped subsonic civil transport aircraft design. *AIAA Journal of Aircraft*, *48*(2), 697–702. https://doi.org/10.2514/1.C031123

Kroo, I. (2001). Drag due to lift: concepts for prediction and reduction. *Annual Review of Fluid Mechanics, 33*, 587–617. https://doi.org/10.1146/annurev.fluid.33.1.587

McMasters, J., & Kroo, I. M. (1998). Advanced configurations for very large transport airplanes. *Aircraft Design, 1*(4), 217–242. https://doi.org/10.1016/S1369-8869(98)00018-4

Munk, M. M. (1923). *The minimum induced drag of aerofoils*. NACA TR-121.

Pate, D. J., & German, B. J. (2013). Lift distributions for minimum induced drag with generalized bending moment constraints. *AIAA Journal of Aircraft, 50*(3), 936–946. https://doi.org/10.2514/1.C032074

Phillips, W. F., Hunsaker, D. F., & Joo, J. J. (2019). Minimizing induced drag with lift distribution and wingspan. *AIAA Journal of Aircraft, 56*(2), 431–441. https://doi.org/10.2514/1.C035027

Prandtl, L. (1921). *Applications of modern hydrodynamics to aeronautics*. NACA TR-116.

Prandtl, L. (1924). Induced drag of multiplanes. From *Technische Berichte*, Vol. III, No. 7. NACA TN-182.

Prandtl, L. (1933). Über Tragflügel kleinster induzierten Winderstandes. *Zeitschrift für Flugtechnik und Motorluftschiffart*, *24*(11), 305–306.

Scardaoni, M. P. (2020). A simple model for minimum induced drag of multiplanes: could Prandtl do the same? *Aerotecnica Missili & Spazio*, *99*(3), 233–249. https://doi.org/10.1007/s42496-020-00058-y

Simmons, G. F. (1992). *Calculus gems: brief lives and memorable mathematics*. McGraw-Hill.

Taylor, J. D., & Hunsaker, D. F. (2020a). Minimum induced drag for tapered wings including structural constraints. *AIAA Journal of Aircraft, 57*(4), 782–807. https://doi.org/10.2514/1.C035757

Taylor, J. D., & Hunsaker, D. F. (2020b). Numerical method for rapid aerostructural design and optimization. In *AIAA Aviation 2020 Forum* (pp. 1–20). Virtual Event. https://doi.org/10.2514/6.2020-3175

Torenbeek, E. (2013). *Advanced aircraft design. Conceptual design, analysis and optimization of subsonic civil airplanes*. Wiley. https://doi.org/10.1002/9781118568101

Whitcomb, R. T. (1976). *A design approach and selected wind-tunnel results at high subsonic speeds for wing-tip mounted winglets.* NASA TN-D-8260.

Wolkovich, J. (1985). The joined wing: an overview. In *AIAA* 23rd *Aerospace Sciences Meeting* (pp. 1–17). Reno, Nevada. https://doi.org/10.2514/6.1985-274

Notations

AR – wing aspect ratio;
b – wingspan (m);
C_d – drag coefficient;
C_{di} – induced drag coefficient;
C_l – lift coefficient;
D_i – induced drag (N);
e – wingspan efficiency factor;
GI – Glauert Integral;
L – lift (N);
$L(y)$ – lift distribution (N/m);
0_a – origin of astroid hypocycloid lift (circulation) distribution;
0_c – origin of combined elliptical and astroid hypocycloid lift (circulation) distribution;
0_e – origin of elliptical lift (circulation) distribution;
V – velocity (m/s);
w – downwash (total induced velocity) due to circulation (m/s);
w_a – induced velocity of outer parts of the wing due to astroid hypocycloid circulation distribution (m/s);
w_{a1} – induced velocity of right outer part of the wing due to astroid hypocycloid circulation distribution (m/s);
w_{a2} – induced velocity of left outer part of the wing due to astroid hypocycloid circulation distribution (m/s);
w_e – induced velocity of center part of the wing due to elliptical circulation distribution (m/s);
y – distance along wing semi-span (m);
y_o – point of induced velocity (downwash) in wing semi-span (m);
Y – factor of semi-span blending position of the two lift distributions;
α_i – induced angle (rad);
Γ_a – astroid hypocycloid circulation (m^2/s);
Γ_e – elliptical circulation (m^2/s);
Γ_{oa} – astroid hypocycloid circulation at origin (m^2/s);
Γ_{oe} – elliptical circulation at origin (m^2/s);
θ – angle in wingspan variable transformation (rad);
θ_o – angle of point of downwash (induced velocity) in wingspan variable transformation (rad);
ρ – density (kg/m^3).

Subscripts

a – astroid hypocycloid;
ac – astroid hypocycloid part of the combination of the two distributions;
c – combined;
d – drag;
di – induced drag;
e – elliptical;
ec – elliptical part of the combination of the two distributions;
l – lift;
∞ – at infinity.